iScience, Volume *24*

Supplemental information

Effects of fixation on bacterial cellular dimensions and integrity

Lillian Zhu, Manohary Rajendram, and Kerwyn Casey Huang

Supplementary Information for "Effects of fixation on bacterial cellular dimensions and integrity"

Authors

Lillian Zhu[1], Manohary Rajendram[1], Kerwyn Casey Huang[1,2,3,*]

Affiliations

[1]Department of Bioengineering, Stanford University, Stanford, CA 94305, USA

[2]Department of Microbiology and Immunology, Stanford University School of Medicine, Stanford, CA 94305, USA

[3]Chan Zuckerberg Biohub, San Francisco, CA 94158, USA

*Corresponding author: kchuang@stanford.edu

Lead author: Kerwyn Casey Huang (kchuang@stanford.edu)

Supplementary Figures

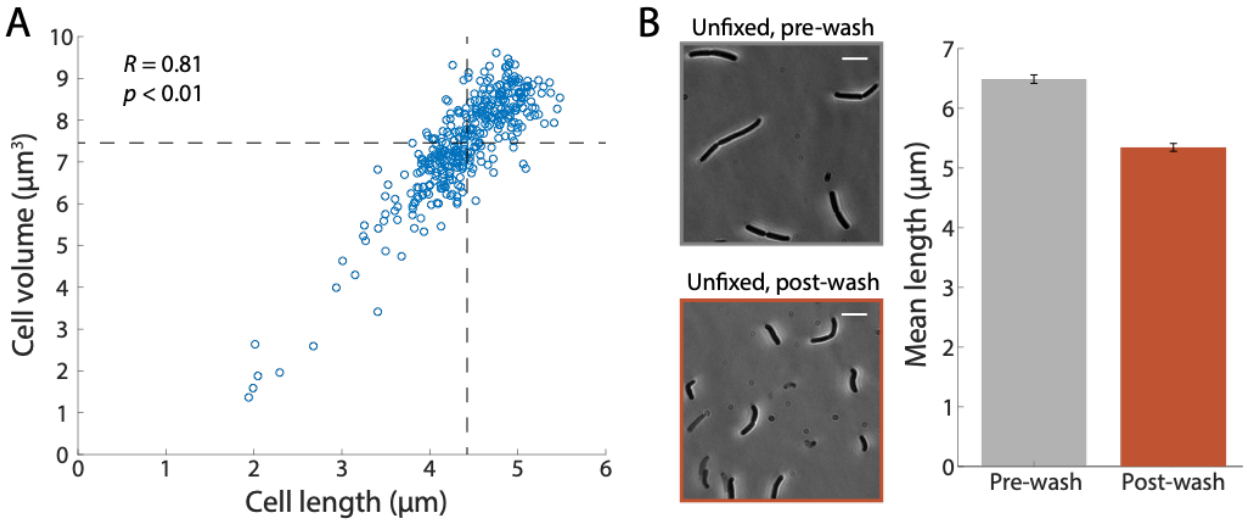

Figure S1: *E. coli* cell length and volume were highly correlated, and washing disrupted *B. subtilis* chaining. Related to Figure 1.

A) Images of unfixed *E. coli* from a single biological replicate were used to segment cell contours. The length and volume of individual cells were highly correlated (n=371 cells).

B) Imaging of unfixed *B. subtilis cells* revealed chaining before but not after washing in PBS (left). Mean cell length was significantly decreased after washing (right). Error bars are 1 standard error of the mean with n=603 and 398 cells for pre- and post-wash, respectively.

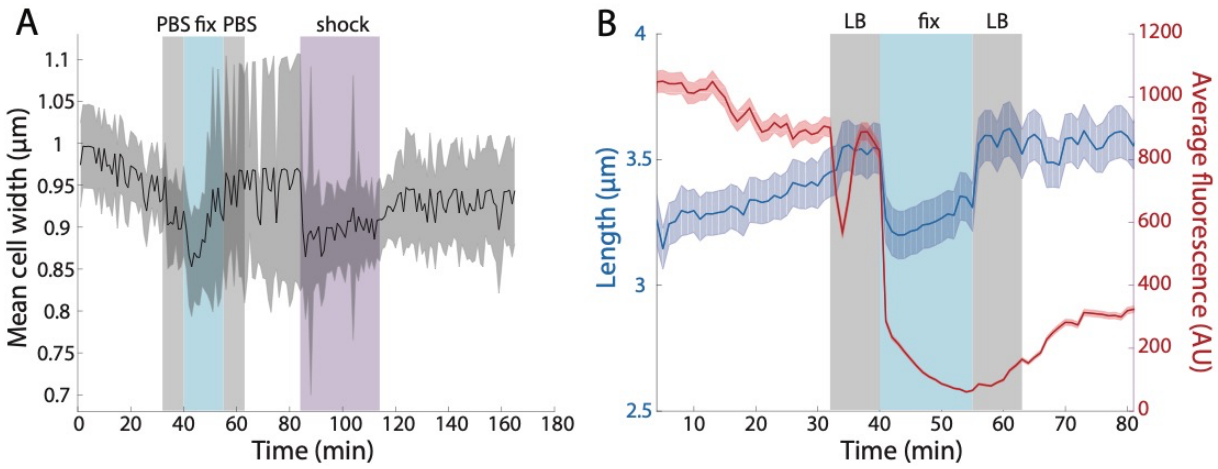

Figure S2: *E. coli* cell width decreases immediately after fixation and during hyperosmotic shock, and fluorescence is not strongly impacted when cells are washed in LB. Related to Figure 2.

A) In the microfluidic flow cell experiment in Fig. 2A, the addition of Chemicon (blue region) caused cell width to initially decrease rapidly, likely due to the loss of material such as fluorescent proteins (Fig. 2A,B); cell width subsequently slowly recovered back to pre-fixation values. Cell width also decreased after the addition of 1 M sorbitol (purple region) and remained low until the sorbitol was removed, indicating that the cell membranes still acted as a semipermeable barrier across which turgor was altered by the shock. The decrease in cell width during the initial 30 min of imaging after loading is likely due to the cells equilibrating to the fixed-height chamber. Curve is the mean of n=150 cells, and gray shaded region represents 1 standard deviation.

B) A microfluidic flow cell experiment involving *E. coli* cells similar to Fig. 2A was carried out with washes in LB rather than PBS. Fluorescence was not strongly impacted during either wash; the transient decrease at the beginning of the first wash was due to focus drift. Curves are means of n=68 cells, and shaded regions represent 1 standard deviation.

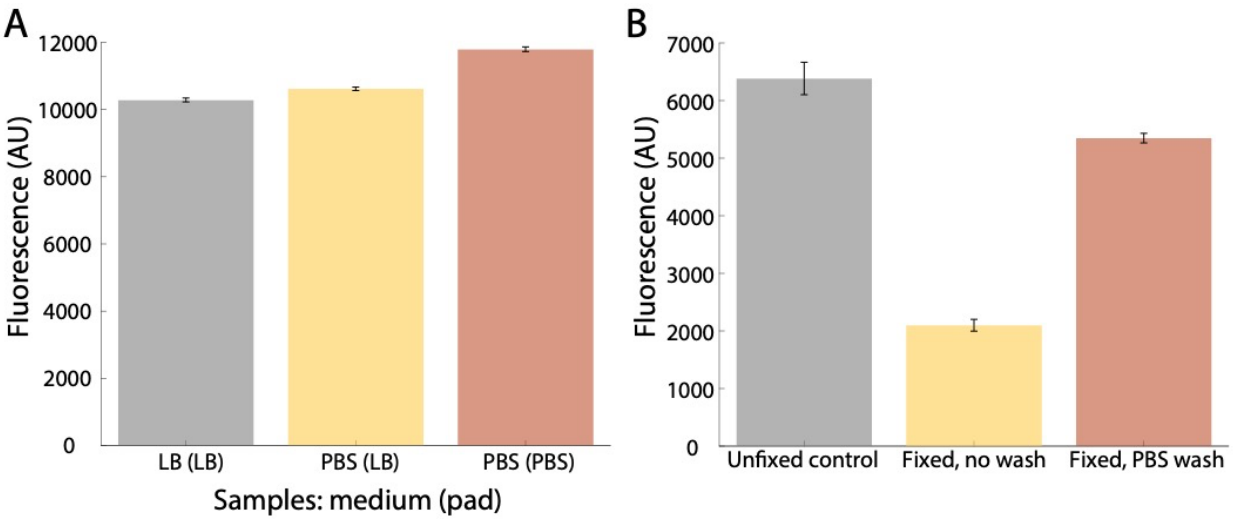

Figure S3: Imaging on PBS pads results in increased fluorescence intensity, particularly after fixation. Related to Figure 3.

A) Log-phase *E. coli* cells grown in LB were imaged on LB-agarose pads before (gray) and after washing in PBS (yellow), or on PBS-agarose pads after washing in PBS (orange). Mean fluorescence intensity was significantly higher on PBS-agarose pads, even accounting for the difference in background fluorescence (Methods). Error bars represent 1 standard error of the mean with n=2160 cells for LB (LB); n=2872 for PBS (LB); n=2571 for PBS (PBS).

B) Log-phase *E. coli* cells were imaged on LB+2% agarose pads directly before fixation, and after fixation in LB+Chemicon without and with a post-fixation wash in PBS. Fluorescence intensity was >2-fold higher in cells after washing in PBS. Data are means over 3 experiments and error bars represent 1 standard error of the mean. Each replicate experiment involved n≥435 cells.

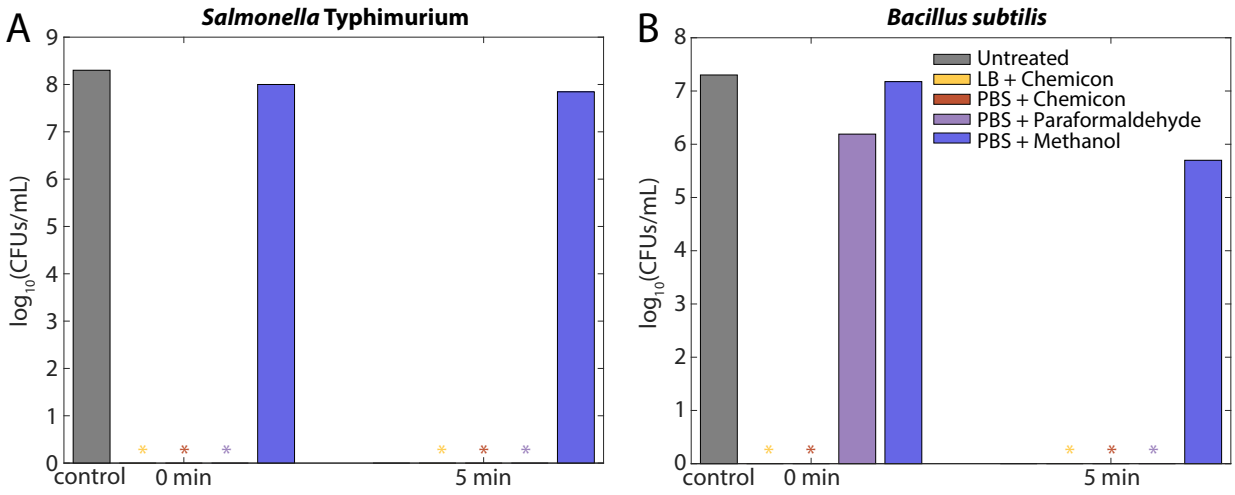

Figure S4: *S.* Typhimurium and *B. subtilis* cells are still able to grow after methanol fixation, while other fixatives halt growth almost immediately. Related to Figure 5.

A,B) Colony forming units (CFUs) of *S.* Typhimurium (A) and *B. subtilis* (B) cells treated for 0 or 5 min with different fixatives. Immediately after resuspension in Chemicon or paraformaldehyde (0 min), *S.* Typhimurium cells plated did not exhibit colony forming ability, and *B. subtilis* cells exhibited a ~10-fold decrease in paraformaldehyde. By contrast, a substantial fraction of cells for both species were able to form colonies after 5 min of methanol fixation. Asterisks indicate that no colonies were observed.

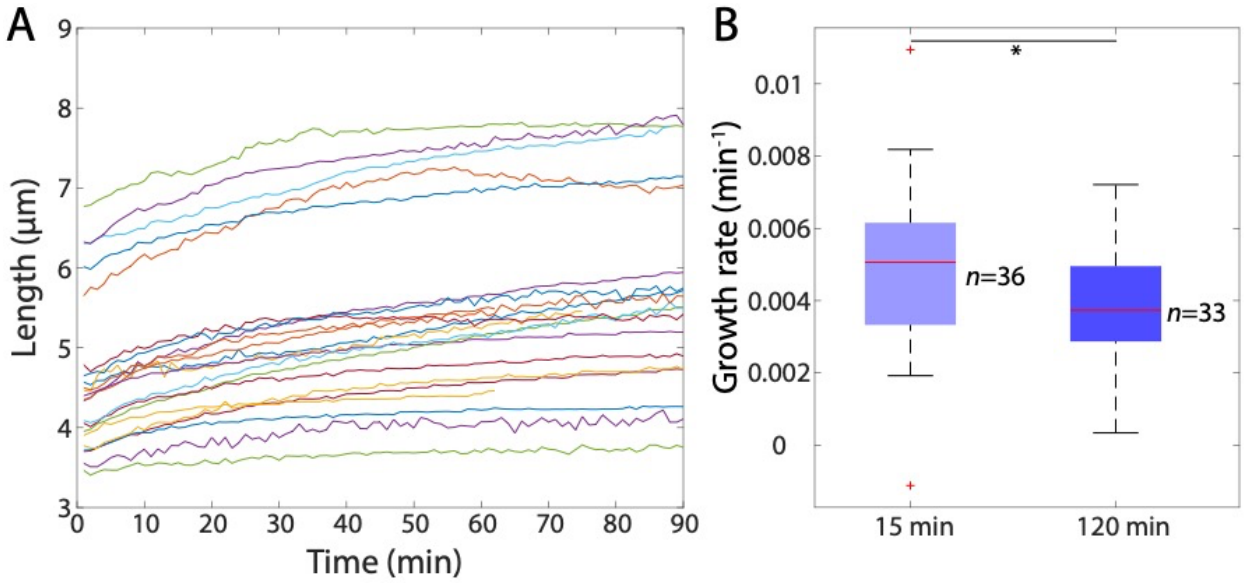

Figure S5: Some *E. coli* cells are still able to grow after 2 hours of methanol fixation. Related to Figure 5.

A) Single-cell growth was impacted by 120 min of methanol fixation. Of the subset of cells that exhibited growth (28 of 105 cells), there was a substantial decrease in growth rate relative to untreated log-phase cells. 22 representative cell traces are shown.

B) Mean growth rate during the first 30 min after fixation was slightly lower after 120 min of methanol fixation compared with 15 min. Growth rate was computed as the amount of elongation per min in the first 30 min, normalized to the initial length (0.01 min^{-1} corresponds to a doubling time of ~70 min). Boxes show the median value and 1st and 3rd quartiles, and error bars extend to the most extreme data points not considered outliers. *: p=0.05.

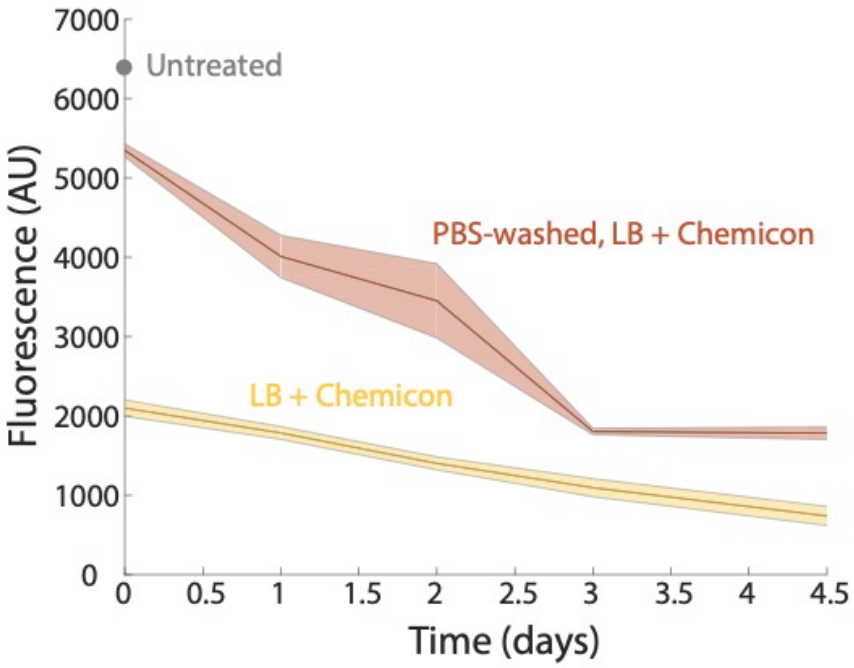

Figure S6: Post-fixation washes in PBS did not impact the decrease in intracellular fluorescence after fixation in LB+Chemicon. Related to Figure 6.

The mean intracellular GFP fluorescence intensity of *E. coli* cells over several days of storage at 4 °C decreased after fixation in LB+Chemicon. If cells were washed in PBS after fixation, fluorescence intensity was higher than in cells that were not washed (similar to Fig. S3), but still decreased over time. Curves are mean values and shaded regions represent 1 standard error of the mean across 3 experiments. Each replicate experiment involved $n \geq 225$ cells.

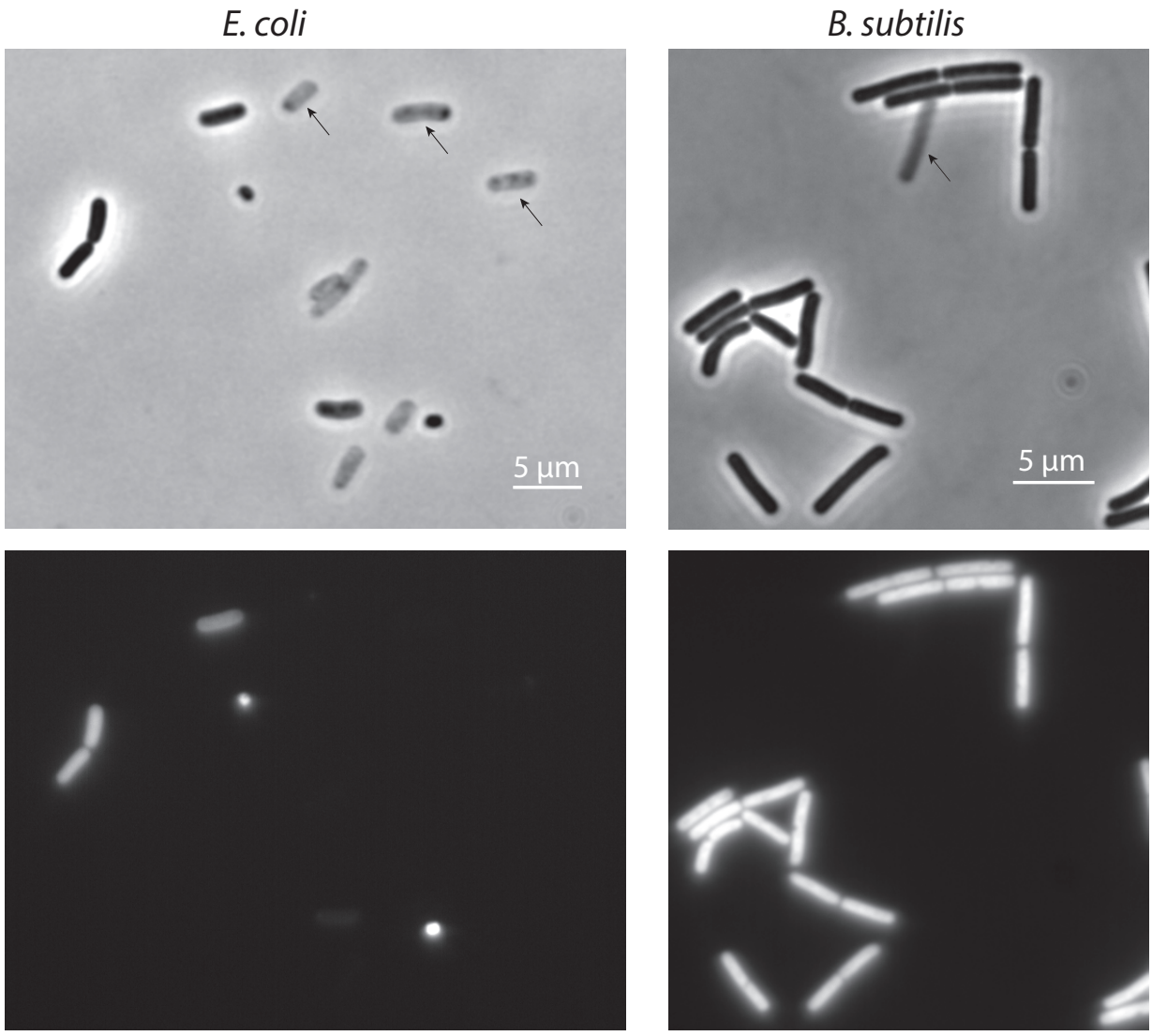

Figure S7: Lysed *E. coli* and *B. subtilis* cells did not retain cytoplasmic fluorescence.

Related to Figure 6.

E. coli cells were fixed with methanol, and *B. subtilis* cells were fixed with formaldehyde.

Cells shown are representative of the population. Arrows highlight selected lysed cells.

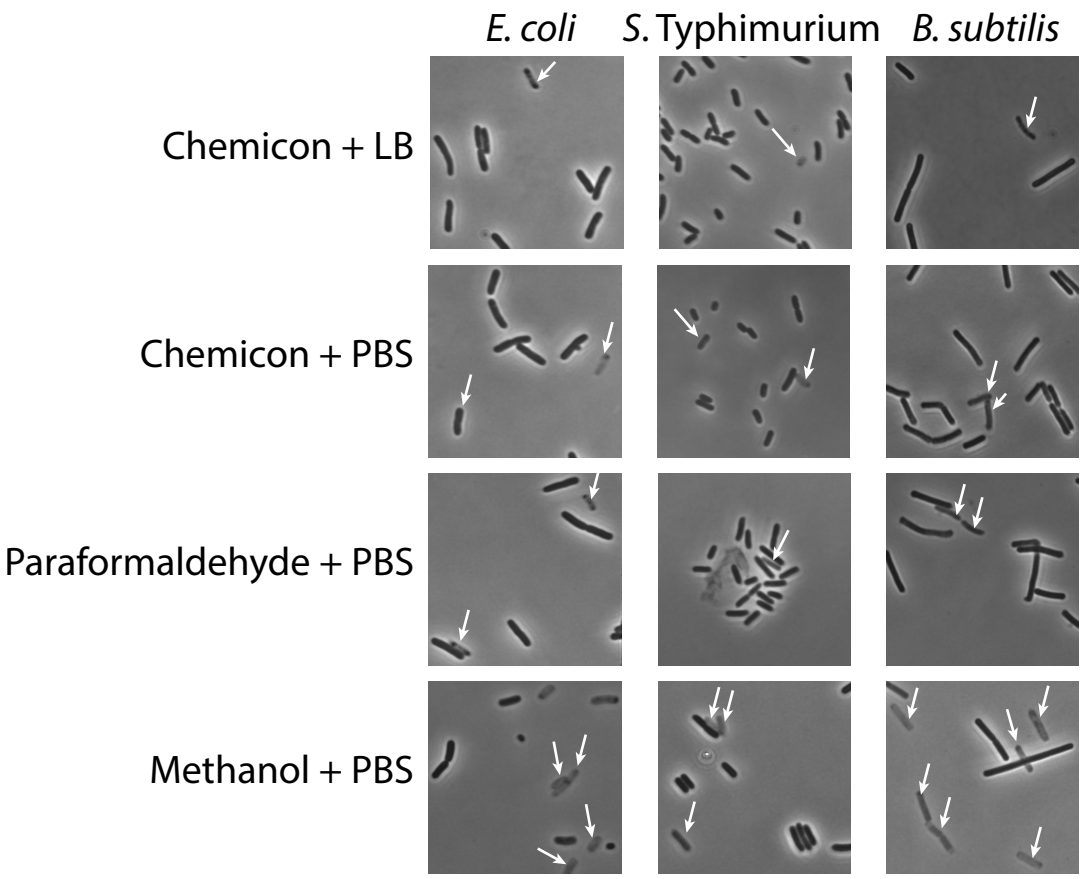

Figure S8: Ghosts were observed in all fixatives. Related to Figure 6.

Representative images of ghosts of *E. coli*, *S.* Typhimurium, and *B. subtilis* cells in each fixation condition.

Transparent Methods

Fixation

Cultures were grown overnight at 37 °C in a shaker at 225 rpm, for 18-20 h. Cultures were then back-diluted 1:100 into fresh LB for 1.5 h at 37 °C. For direct fixation in the LB culture medium, 100 μL of 5X Chemicon were added to 400 μL of culture, and the cells were left for 10 min at room temperature before imaging. To fix in PBS, 1 mL of each culture was apportioned into Eppendorf tubes and spun down at 12,000 rpm for 4 min. The culture medium was aspirated and 1 mL of 1X PBS was added to the tube to resuspend the cells. Cells were pelleted at 12,000 rpm for 4 min and washed once more in 1X PBS. For each condition, 1 mL of fixation medium was added to resuspend the cells, and cultures were left at room temperature for 15 min. Finally, the cells were pelleted and resuspended in 1 mL of 1X PBS for imaging and preservation.

Single-cell imaging

Phase-contrast images were acquired with a Nikon Ti-E inverted microscope (Nikon Instruments) using a 100X (NA 1.40) oil immersion objective and a Neo 5.5 sCMOS camera (Andor Technology). The microscope was outfitted with an active-control environmental chamber for temperature regulation (HaisonTech, Taipei, Taiwan). Images were acquired using μManager v.1.4 (Edelstein et al., 2010). The number of cells

for each sample was determined by total present in the randomly selected fields of view that were imaged.

Microfluidics

Flow-cell experiments were performed in ONIX B04A microfluidic chips (CellASIC) and medium was exchanged using the ONIX microfluidic platform (CellASIC). Overnight cultures were diluted 100-fold into 1 mL of fresh LB and incubated for 1 h with shaking at 37 °C. B04A plates were loaded with medium and primed for 20 minutes. While in the microfluidic chips, the cells were kept at room temperature to mimic the fixation protocol for bulk cultures. Exposure time and fluorescence excitation intensity was kept constant throughout each time-lapse experiment. Incubation in the microfluidic flow cell was at room temperature to match the bulk fixation protocol.

Cell-size analyses

For most images, the Matlab (MathWorks, Natick, MA, USA) image processing code *Morphometrics* (Ursell et al., 2017) was used to segment cells and to identify cell outlines from phase-contrast microscopy images. A local coordinate system was generated for each cell outline using a method adapted from *MicrobeTracker* (Sliusarenko et al., 2011). Cell widths were calculated by averaging the distances between contour points perpendicular to the cell midline, excluding contour points within the poles and sites of

septation. Cell length was calculated as the length of the midline from pole to pole. Cell volume and surface area were estimated from width and length measurements by approximating cells as a pill shape with volume $2\pi R^2(L\text{-}2R) + 4/3\pi R^3$, where R is half the cell width and L is the cell length.

Cellular dimensions (width and length) were quantified by averaging single-cell results across a population. See figure legends for the number of cells analyzed (n) and error bar definitions.

Analysis of fluorescence intensity

Pixel intensities within the contours obtained from Morphometrics segmentation were normalized by subtracting the median background intensity, then summed to determine the total fluorescence. Average fluorescence intensity was defined as the total fluorescence divided by the cell area.

Linear correlation analyses

Pearson's R was calculated for all linear correlation analyses. The p-value for R was calculated using a one-tailed Student's t-test. All n, R, and p-values are included in the corresponding figures and legends.

Code availability

All code is available from the corresponding author upon request

(kchuang@stanford.edu).

Supplementary References

Edelstein, A., Amodaj, N., Hoover, K., Vale, R., and Stuurman, N. (2010). Computer Control of Microscopes Using μManager (John Wiley And Sons, Inc.).

Sliusarenko, O., Heinritz, J., Emonet, T., and Jacobs-Wagner, C. (2011). High-throughput, subpixel precision analysis of bacterial morphogenesis and intracellular spatio-temporal dynamics. Mol Microbiol *80*, 612-627.

Ursell, T., Lee, T.K., Shiomi, D., Shi, H., Tropini, C., Monds, R.D., Colavin, A., Billings, G., Bhaya-Grossman, I., Broxton, M., *et al.* (2017). Rapid, precise quantification of bacterial cellular dimensions across a genomic-scale knockout library. BMC Biol *15*, 17.